DELAMINATION GROWTH MECHANISM FROM EMBEDDED DEFECTS IN COMPRESSION

C.Canturri[1]*, E.S. Greenhalgh[1,] S.T. Pinho[1]S. Nilsson[2]

[1] The Composite Centre, Department of Aeronautics, Imperial College London, London, UK
[2] Swerea SICOMP AB, Molndal, Sweden (earlier at FFA)
* Corresponding author(cc3008@ic.ac.uk)

Keywords: delamination, ply splitting, fractography, compression

1 Introduction

Delamination is a common failure mode in carbon fibre reinforced composites; complex secondary failure modes are frequently associated with it such as fibre failure, matrix cracking and delamination migration. These growth mechanisms need to be understood and predicted to improve structural tolerance to delamination.
To experimentally characterise the behaviour of such delaminations a circular embedded delamination has traditionally been used [1]. Previous experimental studies [2] have focused on the influence of geometrical parameters on the initiation and propagation of the delamination. Numerically, studies have identified the presence of other failure modes in a buckling-driven delamination [3].

In this paper the influence of the orientation of the ply interface on the growth mechanisms is investigated. An experimental procedure has been developed to study the transition of the failure modes while progressively varying the defect interfaces.

2 Experimental

2.1 Mechanical Testing

The specimens studied using SEM were manufactured at DERA from Cytec HTA/919 Tape and tested at FFA (Aeronautical Research Institute of Sweden), details are presented in ref.[4]. Twelve specimens were tested with a quasi-isotropic stacking sequence, $[45^\circ/-45^\circ/0^\circ/90^\circ]_{4s}$, rotated at 0˚, 90˚, 87˚, 85˚, 80˚, 75˚, 65˚ and 45˚. A 10μm thick PTFE film was used to simulate a 50 mm diameter circular defect in the middle a 250 mm x 150 mm plate and between ply interface three and four. To equalise the pressure a 1 mm hole was drilled through the surface to the centre of the delamination plane. Steel end tabs were mounted on the specimens leaving the lateral edges free. Panels were tested in compression, load direction parallel to the 0˚ ply, and were instrumented with strain gauges, whilst a non contact laser gauge was used to detect buckling.
The compressive testing demonstrated that local buckling occurred before global buckling, whereas delamination onset was at a greater load than the panel global buckling load. In all but one of the cases the base laminate buckling direction was backwards (i.e. away from the delamination plane).

2.2 Post mortem analysis- Fractography

For this study, only four specimens were analysed. Their stacking sequence is detailed in Table 1, the insert was situated between the 3rd and 4th plies. To infer the failure modes, directions of growth and delamination failure sequence, the surfaces and the interaction of the different failures mechanisms was studied under a S-3400N Hitachi scanning electron microscope (SEM) at magnifications of between x40 and x1000 with an acceleration voltage of 15 kV, except for Fig. 14 which was studied using a Leo 1550 Field Emission Gun Scanning Microscope.

One side of the resulting delamination was cut-open to give approximately 75 mm x 50 mm specimens and mounted on stubs. Both matching surfaces were gold sputter coated and examined. The zones of interest of both matching surfaces were the insert boundary, where the delamination growth was thought to have started, and all the boundary regions where two different failure modes had interacted.

2.2.1 Description of failure

The baseline specimen chosen for the analyses was specimen L (Table 1), a defect at a 45˚/-45˚ ply interface. This specimen contained most of the failure modes encountered during the whole investigation, i.e. ply splits, delamination migration and fibre failure. In all the specimens, initial optical

inspection identified tide marks visible on the exposed surfaces that matched the delamination fronts seen in the C-scan [2]. The study focused on the interaction between the delamination, splits and translaminar fractures.

45˚/-45˚ ply interface delamination

Firstly, consider the baseline specimen (L) which contained and initial defect at the 45˚/-45˚ interface. Visible inspection (Fig. 1) identified a large ply splits of the 3rd (45˚) and 2nd (0˚) ply and compression failure of the 2nd ply.
Closer SEM examination of the specimen showed further small ply cracks in the 3rd ply all around the insert boundary and extending parallel to the fibres.

Fig. 2 shows a detail of a ply split parallel to ply split A-A' that crossed from the top-left to bottom right separating the image in two distinct zones: the top right region, a fibre rich region, which had failed by mode II dominated delamination and the bottom left, a matrix rich region, with fibre imprints of the adjacent 0˚ ply, which has failed by mode I dominated delamination. The discontinuity of the features encountered on either side of the ply crack indicated the growth of this intralaminar crack had been prior to the formation of the adjacent delaminated surfaces. Furthermore in Fig. 2 the features near the 45˚ ply split suggested that the delamination of the bottommost 0˚/45˚ region had initiated from the ply split.
However, there was some evidence that a number of intralaminar cracks had occurred after the delamination growth (Fig. 3). This region on the insert boundary, near of the delamination onset site, exhibits a mode I dominated delaminated surface. Contrarily to Fig. 2 the features either side of the split were continuous enough to establish that the delamination had been before the ply split.
Fig. 4 was taken close to the intersection of a band of compression failure and the ply splits A-A' and C-C' in Fig. 1. These ply splits A-A' and C-C' may have acted as an initiation site for the 0˚ shear failure pictured in Fig. 4 as its path seemed to have followed the 45˚ ply split, which also present a compression failure.
The same in-plane shear failure then extended into a 0˚ compression failure until reaching ply split B-B' in the 2nd (0˚) ply. Since the compression failure of the 2nd ply was confined between two ply splits (B-B' and C-C' in Fig. 1) it was inferred that these two intralaminar failures had been before the compression failure.
Fig. 5 summarises the sequence of the events for specimen L.

65˚/-25˚ ply interface delamination

The next configuration studied (specimen K) had a stacking sequence that had been rotated through 20˚ with respect to the previous specimen, such that the defect was located at a 65˚/-25˚ ply interface. This specimen exhibited three ply splits (A-A', B-B' and C-C' which resulted in a jump of the delamination interface.
During microscopic observations, further extensive ply splits of the 3rd ply were noted in the matching upper surface that had initiated from the insert and extended in to the rest of the ply. Uniquely, these three ply splits had led to a change of the delamination growth interface. Similarly to specimen L these ply splits (A-A', B-B' and C-C' in Fig. 6) had been prior to the delamination growth. Since these splits were located within the domain of the delamination growth initiation when the delamination front had encountered these ply splits the delamination was prompted to jump.
Fig. 7 shows the boundary of the angled ply split. In this image, the upper region was a 65˚/-25˚ interface whereas the bottom region was a 20˚/65˚ interface. Both regions are matrix dominated and had failed by mode II dominated delamination. The central region of the image shows the flank of the 65˚ ply split which exhibited intralaminar shear cusps. No delamination was observed underneath the ply split which is consistent with the ply split having been present when the delamination had reached that site.
This is similar to the observation in the previous specimen L (45˚/-45˚) where ply splits in the 3rd layer developed both before (Fig. 2) and after (Fig. 3) the delamination growth.
Finally, no compression failure was observed in any of the plies being the only specimen not showing this mode of failure. Nevertheless fibre failure was present; an in-plane shear failure (Fig. 8) between two ply cracks was noted along the insert boundary.
The sequence of failure events is detailed in figure Fig. 9.

80˚/-10˚ ply interface delamination

The next configuration considered was specimen G in which the study sequence had been rotated by 35˚ as compared to the baseline (specimen L, 45˚/-45˚).

The failure surface in specimen G was entirely contained within the defect interface 3rd/4th ply (80˚/-10˚), which had not been observed in specimen L. Ply split A-A' had developed in the 3rd (80˚) ply tangentially to the insert, however its location was distant from the delamination growth initiation sites. Therefore, unlike the baseline (specimen L), no interaction between ply splitting and delamination had occurred. From the absence of delamination beneath 35˚/80˚ ply interface region it was deduced that the ply split A-A' in Fig. 10 had occurred prior to the delamination growth in this zone.
Tangential to the lateral boundary of the defect, a ply split of the 4th (-10˚) ply had developed (B-B' in Fig. 10). From the middle of his ply split a -10˚ compression failure had started to extend away from the defects. Fig. 11 shows the surface of the 4th (-10˚) ply with a visible ply split. On the top left of the image a region of failed fibres can be observed. From the continuity of the fracture morphology it was inferred that the delaminated surfaces were generated prior to the ply split of the 4th (-10˚) ply.
However, compression was after both, delamination and ply splitting, which could be deduced by the presence of the compression failure only one side of the ply split B-B', where compression was thought to have originated. Similarly to specimen L, the compression failure was situated in the ply which was best aligned to the load direction.
Similarly to specimen K (65˚/-25˚), -25˚ in-plane shear failure had developed along the boundary of the insert. This in-plane shear failure was bounded between ply splits of the 4th ply (-10˚).
The sequence of failure events is detailed in figure Fig. 12.

87˚/-3˚ ply interface delamination

The final specimen was rotated 42˚ with respect to the baseline configuration. This specimen presented morphologic similarities with specimen G, it should be noted that they differed in a rotation of 7˚.
Together with specimen G these specimens were the only ones showing fibre failure within the 4th ply. Visually the present failure morphologies were similar; however close examination led to the determination of a different failure sequence. Ply split in the 4th ply (-3˚) was after the translaminar compression failure of the ply contrarily to the observations in specimen G (80˚/-10˚).
This sequence was deduced by the observation that ply splits B-B' and C-C' in Fig. 13 stopped at the compression failure and the similarities in the fracture morphologies either side of the crack in Fig. 14.
The sequence of events is summarised in Fig. 15.

2.2.2 Discussion of failure analysis

Based on the fractographic observations, the general the sequence was deduced to be as follows; a delaminated blister first developed above the defect plane. Due to the high-bending strains at the insert boundary, ply-splits developed and grew along the 3rd ply parallel to the fibres particularly at the transverse boundary where the tensile stresses were higher. When the 3rd ply was approximately orientated at 90˚ the axial bending stiffness at the transverse boundary was increased and therefore the major concentration of the ply splitting was shifted from the transverse boundary to the axial boundary where the bending moment was transverse to the load. This was the case of specimens G and C (80˚/-10˚ and 87˚/-3˚ interfaces) where the ply splits were most concentrated on the axial boundary and therefore did not interact with the delamination front. On the other hand, specimens K and L (45˚/-45˚ and 65˚/-25˚ interfaces), which did not have a 90˚ ply in the blister or had it in the outer plies, exhibited considerable ply splitting around the lateral boundary. The later delamination growth from the embedded defect encountered these cracks, and thus migrated to another interface.
This mechanism was enhanced by the fact that the crack tends to propagate along the upper ply interface [5]. This means that if the upper ply was aligned to the growth direction the delamination would remain in that same interface, which was the case for specimens G and C where the upper ply, was 80˚ and 87˚ respectively. However for specimens K and L, (upper ply being 45˚ and 65˚ respectively) this was not the case. The delamination then migrated through ply splitting until the uppermost ply of the interface matched the growth direction.
After the delamination initiation and growth the generated delaminated surfaces lacked out-of-plane support. The load carrying plies (i.e. 0˚ or close to this) which were at such free surfaces microbuckled and failed. For specimens where there was no predominant load carrier ply, such as in specimen K, compression failure did not develop. Similarly specimens G and C did not have significant load carried within the first three plies and therefore the compression failure was located within the 4th ply (-10˚ and -3˚ respectively).

4 Implications and concluding remarks

Four stacking sequences have been studied in detail and the modes and sequence of failure deduced. Delamination has proven to closely interact with ply splits. Furthermore their position has proven to be of a high importance to allow delamination migration.
The presence of plies parallel to the load would promote the migration and thus inhibit the delamination growth. However, if the delamination was propagating through plies parallel to the load this plies would be in a free surface and thus prone to have an out-of-plane microbuckling, reducing the overall compression strength of the laminate.

Table 1 Stacking Sequence FFA specimens (defect at $3^{rd}/4^{th}$ ply interface)

Specimen	Stacking sequence	Interface
L	$[90^\circ/0^\circ/45^\circ/-45^\circ]_{4s}$	45˚/-45˚
K	$[-70^\circ/20^\circ/65^\circ/-25^\circ]_{4s}$	65˚/-25˚
G	$[-55^\circ/35^\circ/80^\circ/-10^\circ]_{4s}$	80˚/-10˚
C	$[-48^\circ/42^\circ/87^\circ/-3^\circ]_{4s}$	87˚/-3˚

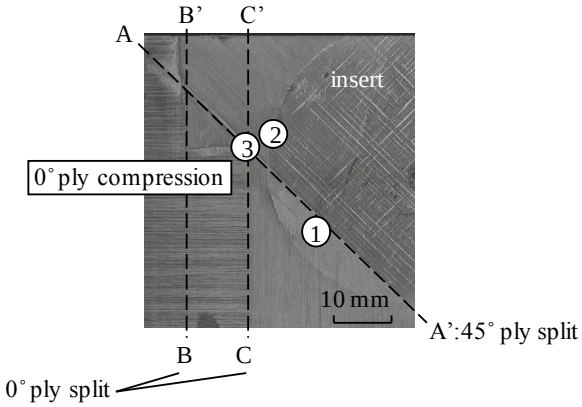

Fig. 1 Lower most fracture surface of specimen L: 45˚/-45˚

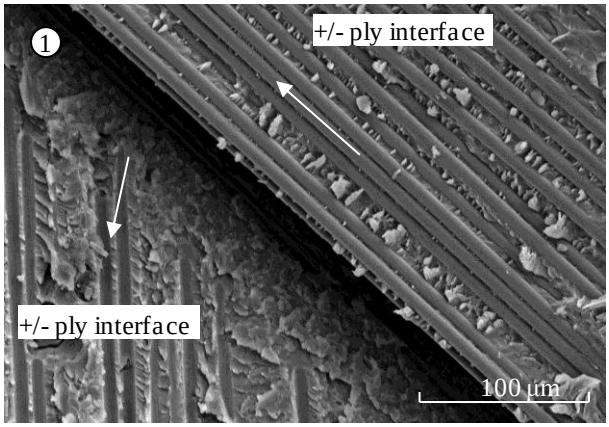

Fig. 2 Ply split of the 45˚ ply

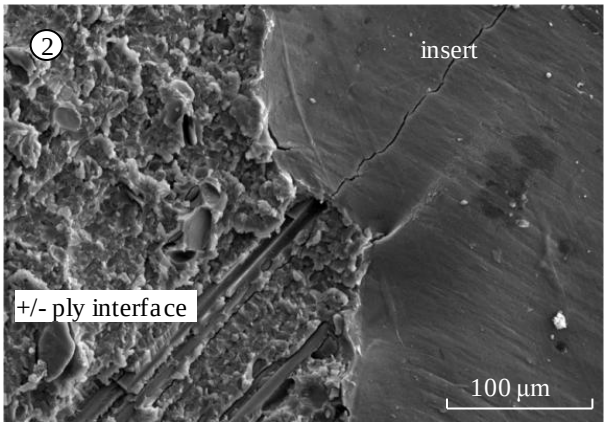

Fig. 3 Ply split of the 45˚ ply. Uppermost matching surface

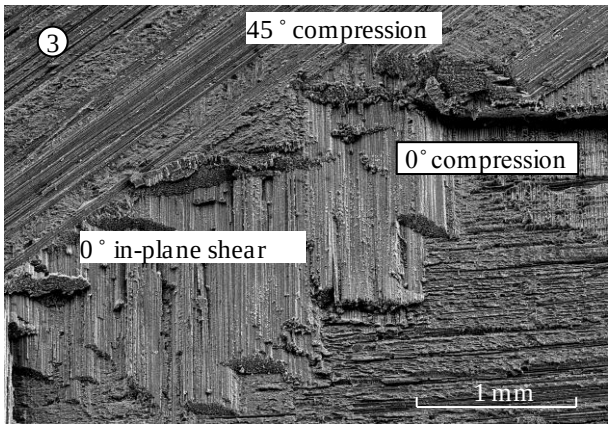

Fig. 4 In-plane shear and compression failure of 45˚ and 0˚ plies. Uppermost matching surface

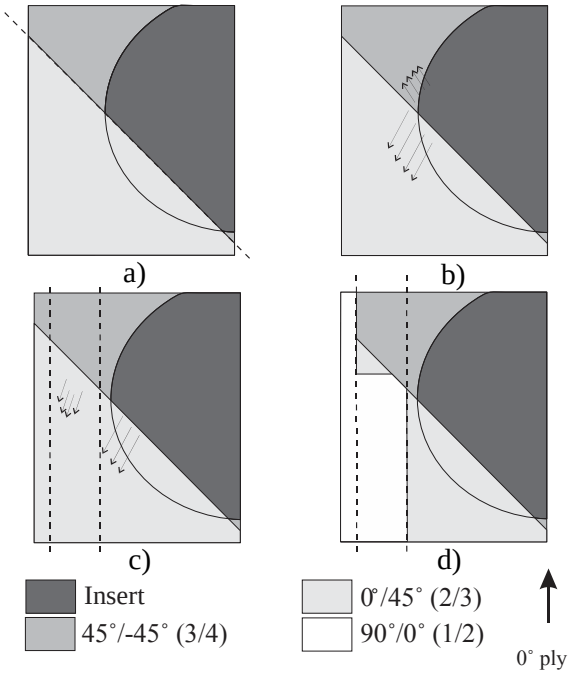

Fig. 5 Failure sequence: ply interface 45˚/-45˚

a) Ply split first develops b) delamination grows on ply interfaces 45˚/-45˚and migrates through the ply split to interface 0˚/45˚ c) ply splits develop in the 0˚ layer d) in-plane shear failure and compression failure of the 0˚

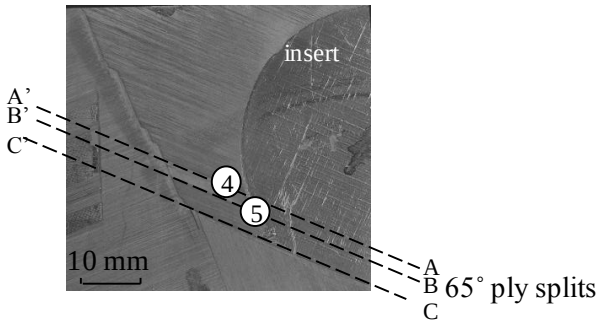

Fig. 6 Lowermost failure surface of specimen K: 65˚/-25˚

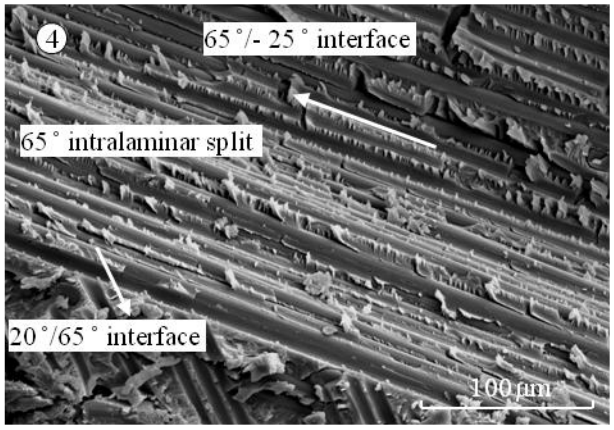

Fig. 7 Flank of 65˚ ply slit

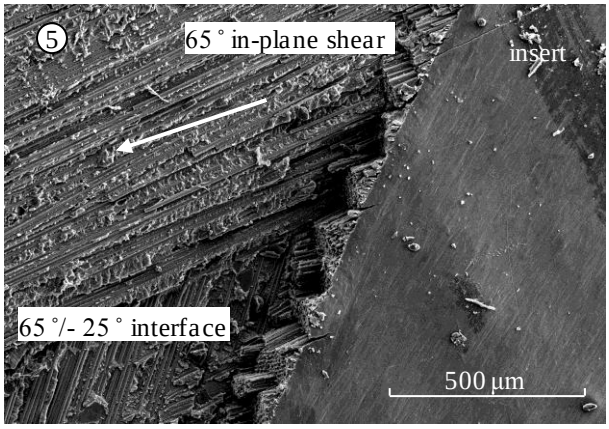

Fig. 8 Boundary of the insert showing an in-plane shear failure. Upper most matching surface.

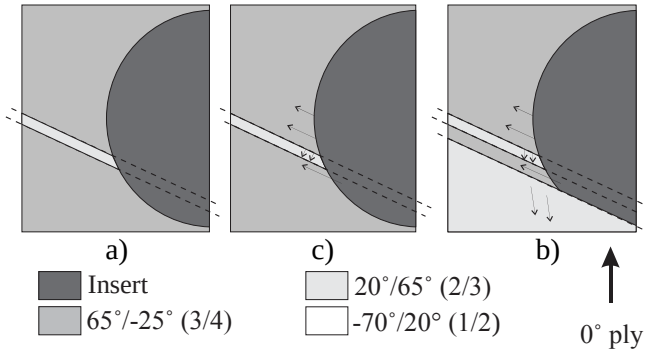

Fig. 9 Failure sequence specimen L: ply interface 65˚/-25˚

a) Ply splits first develop in the 65˚ ply b) delamination grows on ply interfaces 65˚/-25˚and migrates through the ply split to interface 20˚/65˚ c) ply splits develop in the -70˚ layer

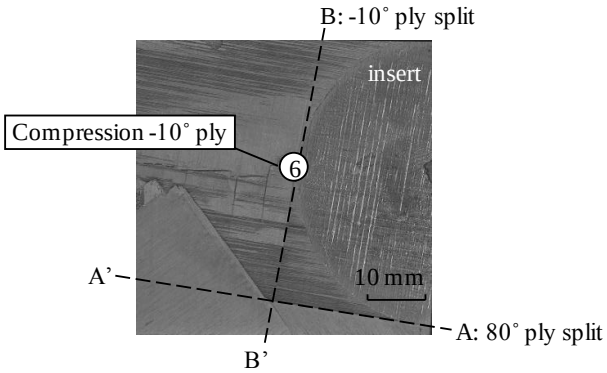

Fig. 10 Lowermost failure surface of specimen G: 80˚/-10˚

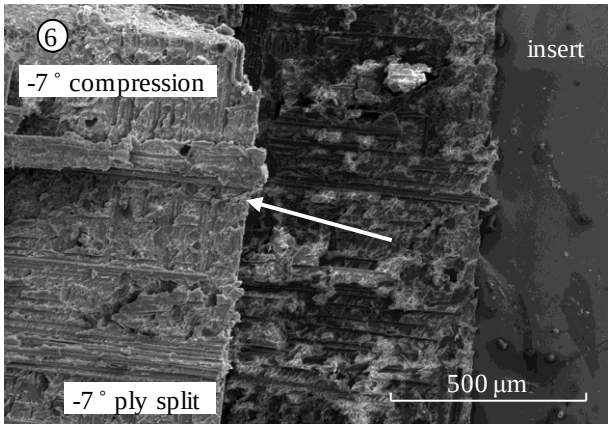

Fig. 11 Boundary of the insert showing compression failure and ply split of the -10˚ ply.

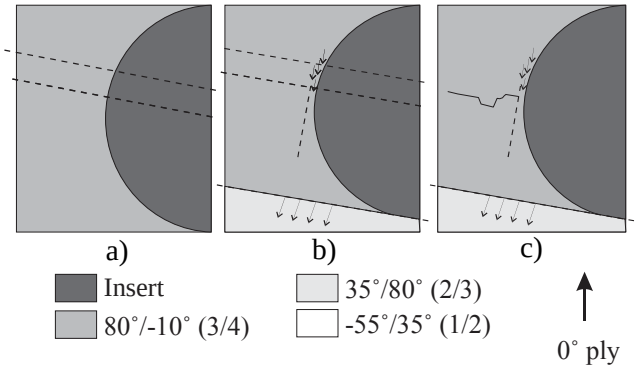

Fig. 12 Failure sequence specimen L: ply interface 80˚/-10˚

a) Ply splits first develop in the 80˚ ply b) delamination grows on ply interfaces 80˚/-10˚, ply -10˚ splits c) compression failure of the -10˚ ply

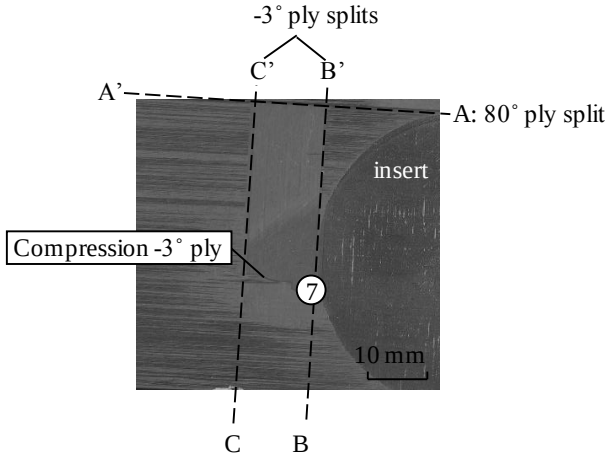

Fig. 13 Lowermost failure surface of specimen C

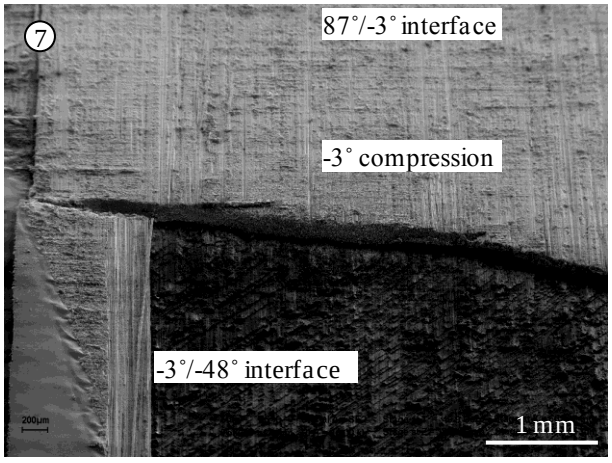

Fig. 14 Boundary of the insert showing compression failure and ply split of the -3˚ ply. Image rotated 180˚

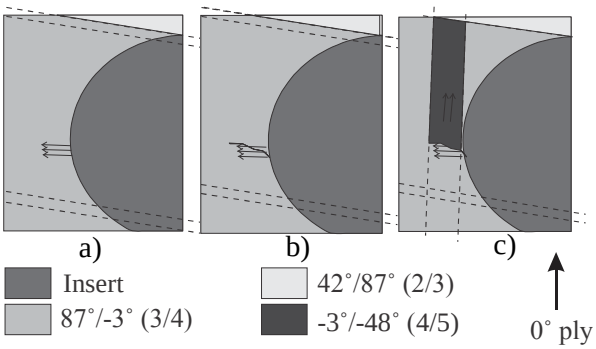

Fig. 15 Failure sequence specimen L: ply interface 87˚/-3˚

a) Ply splits develop in ply 87˚ and delamination grows on ply interfaces 87˚/-10˚ b) compression failure of the -3˚ ply c) ply splits on the -3˚ ply

References

[1] H. Chai, W.G. Knauss, C.D. Babcock "Observation of damage growth in compressively loaded laminates". *Journal of Experimental Mechanics*, Vol. 23, No. 3, pp 329-337, 1983

[2] K.-F. Nilsson, L.E. Asp and A. Sjögren "On transition of delamination growth behaviour for compression loaded composite panels". *International Journal of Solids and Structures*, Vol. 38, pp 8407- 8440, 2001.

[3] A. Riccio, e. Pietropaoli "Modelling damage propagation in composite plates with embedded delamination under compressive load" *Journal of Composite Materials*, Vol. 42 pp 1309-1335, 2008

[4] S. Nilsson "Compression test of composite panels with embedded delaminations". FFA TN 2000-74

[5] ES. Greenhalgh, C. Rogers, P. Robinson "Fractographic observations on delamination growth and the subsequent migration through the laminate" *Composite Science and Technology*, Vol. 69, No. 14, pp 2345-2351, 2009